

Numerical Investigation of Monitoring Antenna Influence on Shielding Effectiveness Characterization

T. Cvetković¹, V. Milutinović¹, N. Dončov², and B. Milovanović²

¹ Republic Agency for Electronic Communications
Belgrade, 11000, Republic of Serbia
tatjana.cvetkovic@ratel.rs, vesna.milutinovic@ratel.rs

² Faculty of Electronic Engineering
University of Niš, Niš, 18000, Republic of Serbia
nebojsa.doncov@elfak.ni.ac.rs, bratislav.milovanovic@elfak.ni.ac.rs

Abstract — This paper deals with an impact of receiving antenna placed in a metal enclosure on an electromagnetic field distribution within the enclosure, and thus on its shielding effectiveness. In an experimental setup, a frequently used tool for measuring the electromagnetic field level at certain points within the enclosure is a dipole antenna connected to a measuring instrument via a coaxial cable. For modeling a coupling between the electromagnetic field and antenna in the protective enclosure we use the Transmission-Line Matrix (TLM) method, enhanced with the compact wire model. The numerical model is verified through comparison with the available experimental results and then used to investigate the influence of physical dimensions of dipole antenna and its cable connection on the detected level of shielding effectiveness.

Index Terms — Dipole antenna, enclosure, shielding effectiveness, TLM wire model.

I. INTRODUCTION

For correct operation of electronic equipment, its proper protection is of key significance. Metal enclosures represent the most frequent form of protection. The performances of any electronic system placed in a protective enclosure, in terms of Electromagnetic Compatibility (EMC) [1], depend on the character of the source of external/internal Electromagnetic (EM) radiation, the configuration of wire and dielectric structures within the system, as well as the existence and

nature of coupling paths, through which the coupling of EM source energy and sensitive parts of the electronic system is realized. The performance of metal enclosures is usually assessed by the Shielding Effectiveness (SE), defined as a ratio between the field strength with and without an enclosure, at the same observed point. The value of this parameter, and thus the entire resistance of the system, depends on the structure and form of the enclosure and characteristics of the materials the enclosure is made of.

In practical use, there are apertures on the enclosure walls whose purpose is the access to the system and its control, laying of power supply and by-pass cables, ventilation, cooling, etc. EM radiation penetrating through the apertures has an adverse effect on the enclosure's protective function. It is therefore necessary to perform an analysis and determine the nature and level of the EM emission originating from different parts of the system, as well as the impact of externally generated EM disturbances on the functionality of the overall system; i.e., to determine the enclosure SE and undertake steps for elimination/reduction of coupling paths.

Numerous techniques are currently available for the calculation of the SE, from analytical methods to numerical simulations. Analytical methods represent fast tools, but their application is usually limited to simplified problems. One of analytical approaches used the Mendez method based on solving the problem of scattering [2].

Analytical solution based on an equivalent waveguide circuit was proposed in [3] and enhanced in [4] to allow for considering oblique incidence and polarization of incident plane wave and arbitrary location of apertures on enclosure walls. The numerical methods were also used for the SE calculation; e.g., the Finite Difference Time Domain (FDTD) method in [5], the Methods of Moments (MoM) in [6] and the Transmission Line Matrix (TLM) method in [7,8,9]. Various factors, such as aperture patterns (dimensions, number and orientation of apertures) and plane wave excitation parameters, and their impact on shielding properties of enclosure have been numerically considered at high frequencies.

The shielding performances of enclosure may also be characterized by experimental measurements. In that case, a small receiving dipole antenna is placed within the enclosure in order to measure the level of EM field at some characteristic points. Antenna is connected via a coaxial cable to an instrument that records measurement results (most frequently it is a network analyzer). Antenna of finite dimensions could significantly affect the EM field distribution in closed environment as already shown in [10] for resonant cavity-based microwave applicators. It is also mentioned in [4] as an explanation for some differences between the results obtained by presented equivalent circuit model, which does not include antenna presence, and the experimental SE results.

Therefore, the aim of this paper is to numerically investigate the influence of dipole antenna during experimental procedure for SE characterization. The TLM method is used here as a numerical tool due to the integrated solution introduced in this method in the form of compact wire model [11] and later extended in [12] for cylindrical mesh. Such enhanced TLM method allows to create a numerical model capable to efficiently take into account the dipole presence without resorting to an extremely fine mesh and to describe its two-way coupling with the EM field inside the enclosure. The model is first verified through comparison with the available experimental SE results for a rectangular enclosure with various rectangular apertures on its front wall [4]. Then it is used to calculate the SE of enclosure considering different physical dimensions of dipole antenna and its cable connection in order to

analyze their impact on detected EM field level.

II. TLM MODELING OF ENCLOSURE WITH DIPOLE ANTENNA INSIDE

The TLM method [13] is a numerical modeling technique based on temporal and spatial sampling of EM fields. In the TLM method, a Three-Dimensional (3D) EM field distribution in enclosure is modeled by filling the space with a network of transmission link lines. EM properties of a medium inside the enclosure are described by using a network of interconnected nodes. A typical node structure is the Symmetrical Condensed Node (SCN), which is shown in Fig. 1. Additional stubs are attached to SCN to model inhomogeneous and lossy materials and/or a modified SCN, so-called hybrid SCN [13] is usually used to operate simulations at a higher time-step. External boundaries of arbitrary reflection coefficient of enclosures are modeled in the TLM by terminating the link lines at the edge of the problem space with an appropriate load. Individual apertures on enclosure walls are usually described by a finer mesh; i.e., using several TLM nodes across each aperture dimension, while in the case of higher number of apertures, so-called airvent model [8] can be used.

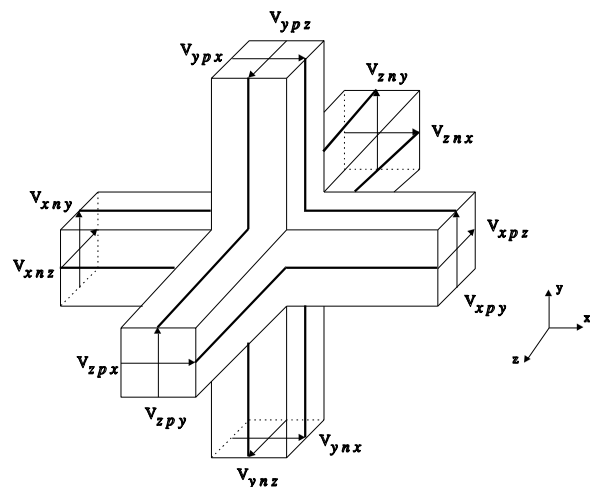


Fig. 1. Symmetrical condensed node.

Wire structures inside the enclosure can be efficiently represented by a compact TLM wire model [11], which considers wires as new elements that increase the capacitance and inductance of the medium in which they are

placed. This model allows for accurate modeling of wires with a considerably smaller diameter than the node size. It uses a special wire network formed by additional link and stub lines (Fig. 2) whose characteristic impedance parameters, Z_w and Z_{ws} , are chosen to model the capacitance and inductance increased by the wire presence, while at the same time maintaining synchronism with the rest of the transmission line network. This wire network is embedded within the TLM nodes (Fig. 3) to model signal propagation along the wires, while allowing for interaction with the EM field. Coupling between the additional link and stub lines with the rest of the TLM node is achieved through points A and B.

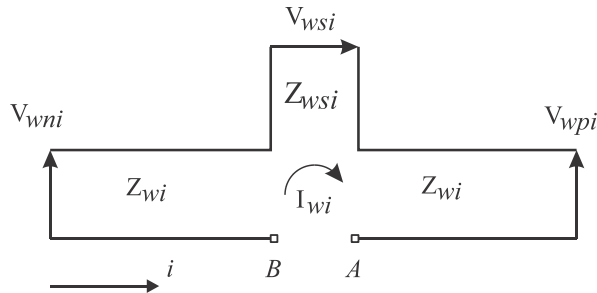


Fig. 2. Wire network for a straight wire running in the i -direction.

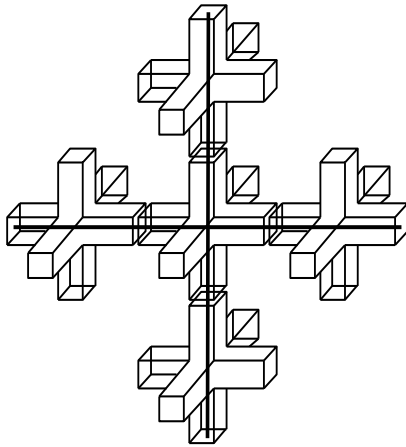


Fig. 3. Wire network embedded within the TLM nodes.

The single column of TLM nodes, through which wire conductor passes, can be used to approximately form the fictitious cylinder which represents capacitance and inductance of wire per

unit length. Its effective diameter, different for capacitance and inductance, can be expressed as a product of factors empirically obtained by using known characteristics of TLM network and the mean dimensions of the node cross-section in the wire running direction [11].

For an example, for the node containing i -directed straight wire segment, as depicted in Fig. 2, the effective diameters of fictitious cylinder for wire capacitance and inductance can be defined as:

$$d_{Ci} = 2k_{Ci}\Delta i_c, \quad (1)$$

$$d_{Li} = 2k_{Li}\Delta i_c, \quad (2)$$

respectively, where Δi_c represents mean cross-section dimensions of the TLM node in i direction, $\Delta i_c = (\Delta j + \Delta k)/2$. Empirically found factors k_{Ci} and k_{Li} for the wire located in free space are:

$$k_{Ci} = 0.0511k_i^2 + 0.0194k_i + 0.617, \quad (3)$$

$$k_{Li} = 0.34, \quad (4)$$

and for the wire above the ground:

$$k_{Ci} = 0.0223k_i^2 + 0.024k_i + 0.606, \quad (5)$$

$$k_{Li} = 0.347. \quad (6)$$

Parameter k_i depends on time- and space-step discretization and EM properties of medium represented by the TLM node and it can be calculated as:

$$k_i = 2\Delta t / (\sqrt{\epsilon\mu}\Delta i_c). \quad (7)$$

Once the effective diameters are known, the per-unit length wire capacitance and inductance can be calculated as:

$$C'_{wi} = 2\pi\epsilon / \ln(d_{Ci} / d_w), \quad (8)$$

$$L'_{wi} = \mu \ln(d_{Li} / d_w) / 2, \quad (9)$$

where d_w is a real wire diameter. Wire per-unit length capacitance is then modeled by the link line of characteristic impedance Z_{wi} :

$$Z_{wi} = \frac{\Delta t}{\Delta i C'_{wi}}, \quad (10)$$

while the wire per-unit length inductance is modeled by short-circuit stub of characteristic impedance Z_{wsi} :

$$Z_{wsi} = L'_{wi} \frac{\Delta i}{\Delta t} - Z_{wi}. \quad (11)$$

Resistive load termination at the end of wire can be treated in two ways. In the first case, lossy termination is shifted to the centre of the last wire segment, causing changes in scattering procedure of the wire node. Also, resistive load can be

defined exactly at the wire end, and in that case, a Thevenin equivalent circuit (Fig. 4) is used to determine the required reflection coefficient. A resistor R is used to connect one end of wire to a nearby ground or metal. The required reflection coefficient ρ for this wire termination is given by:

$$\rho = \frac{R - Z_{wi}}{R + Z_{wi}} \quad (12)$$



Fig. 4. Resistive load termination at one wire end.

All the mentioned models are incorporated into 3D SCN TLM mesh and implemented in 3D TLMscn solver, developed at the Microwave Lab at the Faculty of Electronic Engineering in Nis, Serbia.

III. NUMERICAL ANALYSIS

Impact of receiving dipole antenna on the SE is considered here, on the example of rectangular enclosure with dimensions: $l_x=300$ mm, $l_y=400$ mm and $l_z=200$ mm (Fig. 5). The frontal wall of the enclosure is made of 2 mm thick Al conducting material with different patterns and numbers of rectangular apertures as shown in Fig. 6. A plane wave of normal incidence to the frontal panel and with vertical electric polarization is used as an excitation. Choice of enclosure geometry, aperture dimensions and patterns, excitation and output was governed by experimental arrangements in [4].

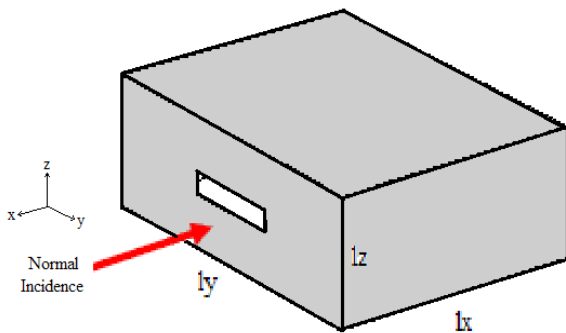


Fig. 5. Enclosure with a rectangular cross-section.

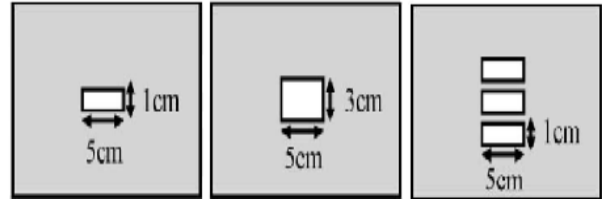


Fig. 6. Frontal panel with one or three apertures of different size.

First, it is assumed that the space inside the enclosure is empty. TLM method is used to calculate the level of EM field with and without enclosure. The frequency dependence of the SE for all aperture patterns is presented in Fig. 7.

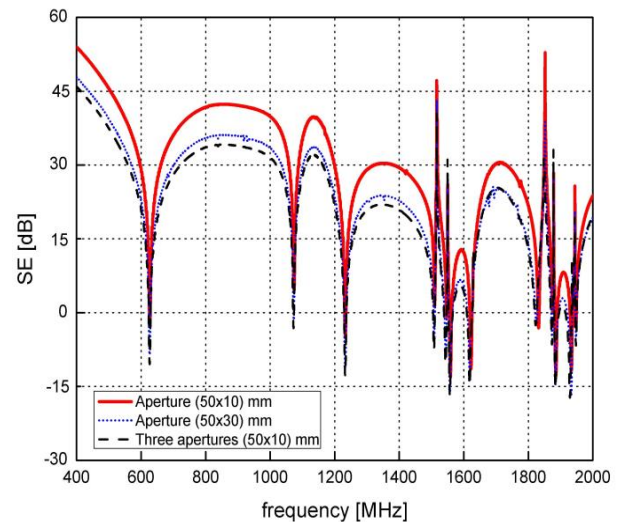


Fig. 7. SE of enclosure with various aperture patterns on the front wall-TLM model of enclosure without antenna.

As it can be seen from Fig. 7, the shape of the SE curve is similar for all considered patterns of apertures, including the values of resonant frequencies. This indicates that the patterns and the number of apertures mostly affect the level of attenuation to which EM field propagating through apertures is exposed. As expected, the level of the SE decreases with the increase of area covered by apertures. It should be also pointed out that the numerical results are in good agreement with the results obtained by equivalent circuit model presented in [4], as it can be seen from Fig. 8 for an aperture (50x10 mm). Similar agreement is obtained for the other two aperture patterns.

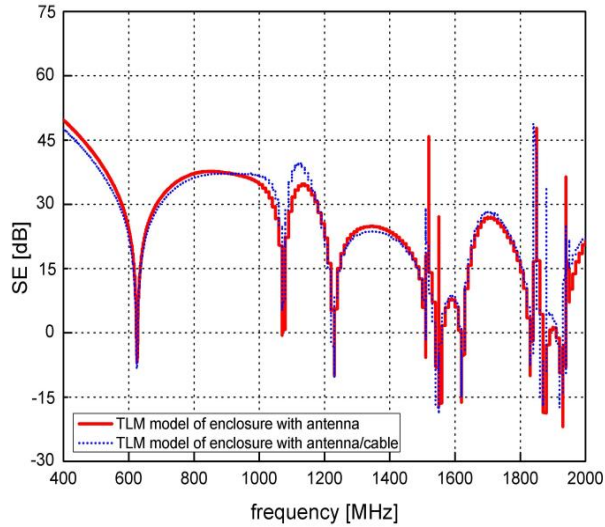


Fig. 8. SE of enclosure with one aperture (50x10 mm) on the front wall-TLM model of enclosure without antenna and equivalent circuitual model presented in [4].

Further, the physical presence of the dipole antenna in the enclosure is considered, as well as the impact of the different radii of the dipole antenna on the SE of the enclosure. For this SE calculation, the compact wire model described in Section II is used to model the dipole antenna. Dipole antenna is represented as two z-directed 50 mm long wires, both having the radius of 0.1 mm, and mutually separated by 2 mm. Their position within the enclosure is defined at the point slightly off the enclosure center in x-direction as specified in [4]. The electric field is directly taken at the point in space between two wires instead of picking up signal directly from the antenna. The SE results obtained by TLM simulations are compared to the experimental results [4] and shown in Figs. 9-11. Good agreement between numerical and experimental results can be observed.

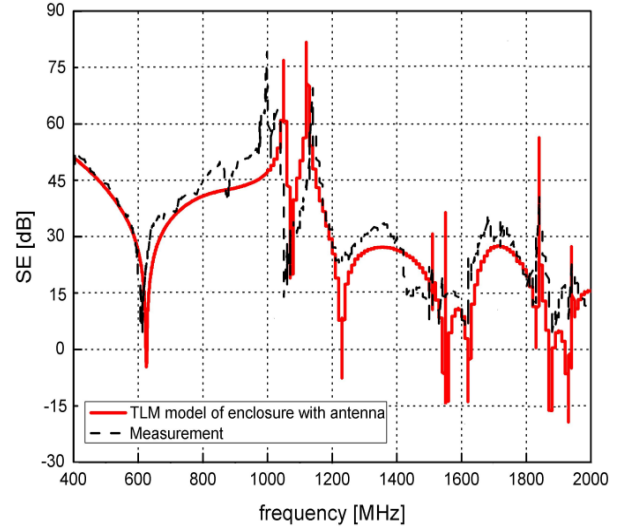


Fig. 9. SE of enclosure with one aperture (50x10 mm) on the front wall-TLM model of enclosure with antenna and measurements [4].

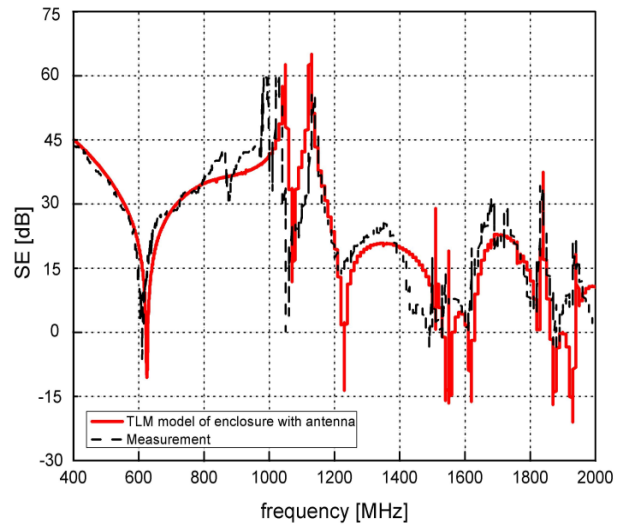


Fig. 10. SE of enclosure with one aperture (50x30 mm) on the front wall-TLM model of enclosure with antenna and measurements [4].

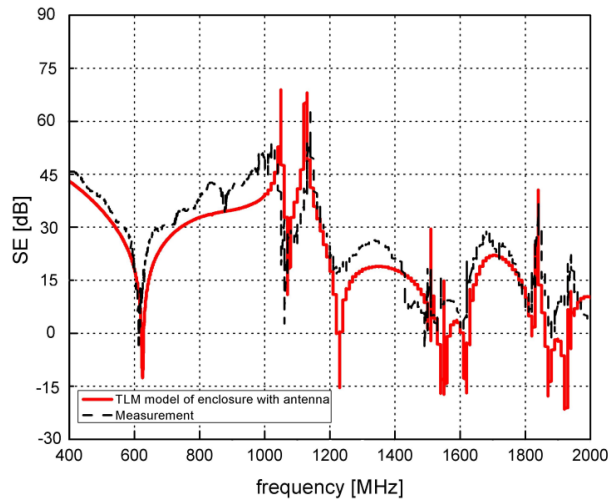


Fig. 11. SE of enclosure with three apertures (50x10 mm) on the front wall-TLM model of enclosure with antenna and measurements [4].

The SE results obtained by TLM simulations for different radii of dipole antenna within the enclosure with one aperture (50x10 mm) on the front wall are shown in Fig. 12. It can be noticed that the level of the SE decreases with the increase of wire radius while the resonant frequencies shift towards lower frequencies. When wire radius is decreasing, the resonant frequencies are approaching to the case when antenna is excluded from the numerical model. Values of the first resonant frequency for different radii of the antenna are given in Table 1.

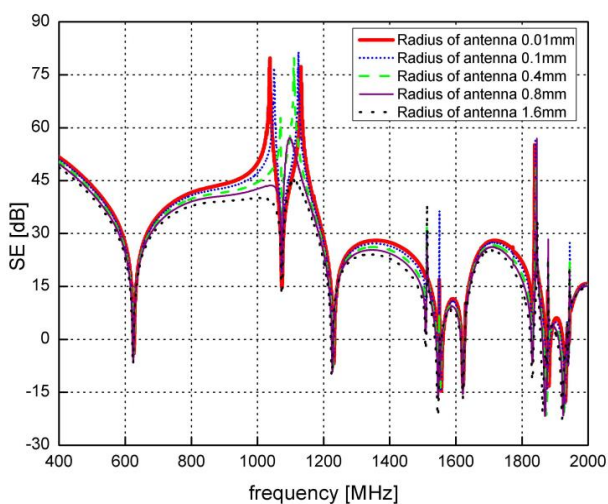


Fig. 12. Impact of the increase of wire radius on the SE of enclosure with one aperture (50x10 mm) on the front wall.

Table 1: Value of the first resonant frequency for different radii of the dipole antenna

Radius of Antenna (mm)	First Resonant Frequencies (MHz)
0.001	626.095
0.1	625.600
0.4	624.981
0.8	624.485
1.6	623.619

The SE results obtained by TLM simulations for different length of dipole antenna of radius 0.1 mm within enclosure with one aperture (50x10 mm) on frontal wall are shown in Fig. 13. The same effects can be observed as in the case of different wire radii. Level of the SE decreases and the resonant frequencies shift toward lower frequencies with the increase of antenna length, due to stronger influence of antenna as a second emitter on total EM field inside the enclosure. Change of antenna length also influences the location of the first dipole antenna resonance. The same conclusions regarding the impact of physical dimensions of the antenna on the SE can be reached if the TLM method enhanced with wire model is applied to the enclosure with other considered aperture patterns on the front wall.

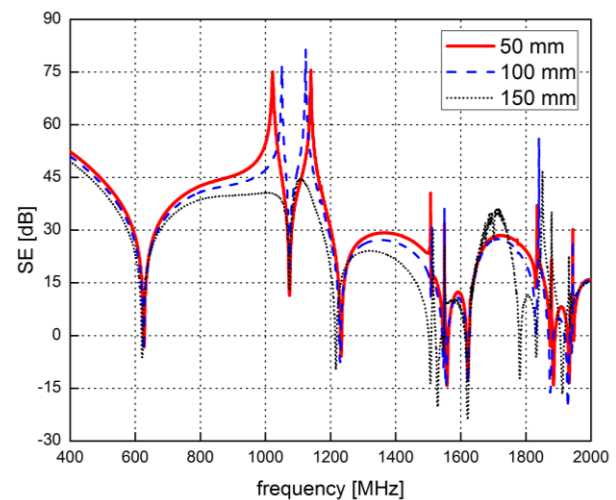


Fig. 13. Impact of the increase of wire length on the SE of enclosure with one aperture (50x10 mm) on the front wall.

The same effects can be observed as in the case of different wire radii. Level of the SE

decreases and the resonant frequencies shift toward lower frequencies with the increase of antenna length due to stronger influence of antenna as a second emitter on total EM field inside the enclosure. Change of antenna length also influences the location of the first dipole antenna resonance. The same conclusions regarding the impact of physical dimensions of the antenna on the SE can be reached if the TLM method enhanced with wire model is applied to the enclosure with other considered aperture patterns on the front wall.

In previous cases, the SE is calculated based on the EM field level directly taken in space between two wires. However, during the experimental measurement of the SE, signal is picked up directly from the antenna and via a coaxial cable transferred to the network analyzer. In order to create a numerical model that will correspond to the experimental case, both 50 mm long wires of 0.1 mm radius are connected in their mutually nearest points by resistor R equal to the impedance of the coaxial cable. Physical presence of coaxial cable is not taken into account as cable can be placed in such position (closed to enclosure wall and with minimal running length) not to disturb the EM field distribution inside the enclosure. Impact of balun usually placed between antenna and cable is also neglected.

Current induced in the dipole antenna is shown in Fig. 14 for the case of the enclosure with three apertures (50x10 mm) on the front wall. It can be used to find the voltage induced between wires ends; i.e., in the centre of the dipole antenna, with and without the enclosure in order to calculate the SE.

Numerical results for the SE together with the results of the case when only dipole antenna is considered (without the cable connection) and experimental results are shown in Figs. 15-17. The position of the dipole antenna is the same as in the

previously considered case.

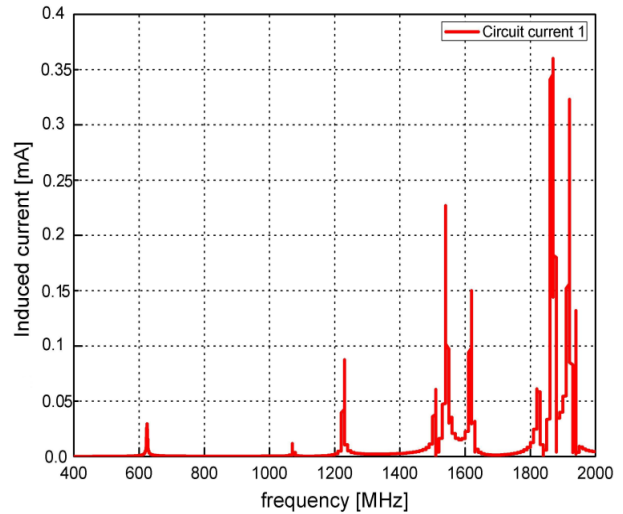


Fig. 14. Induced dipole antenna current as a function of frequency.

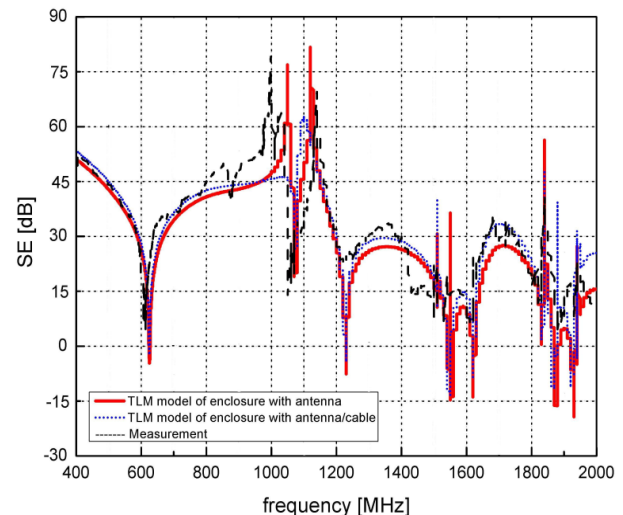


Fig. 15. SE of enclosure with one aperture (50x10 mm) on the front wall-TLM models of enclosure with antenna/cable and with antenna and measurements [4].

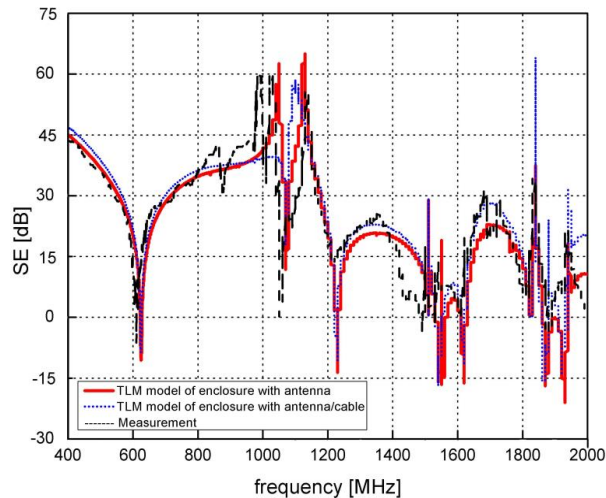


Fig. 16. SE of enclosure with one aperture (50x30 mm) on the front wall-TLM models of enclosure with antenna/cable and with antenna and measurements [4].

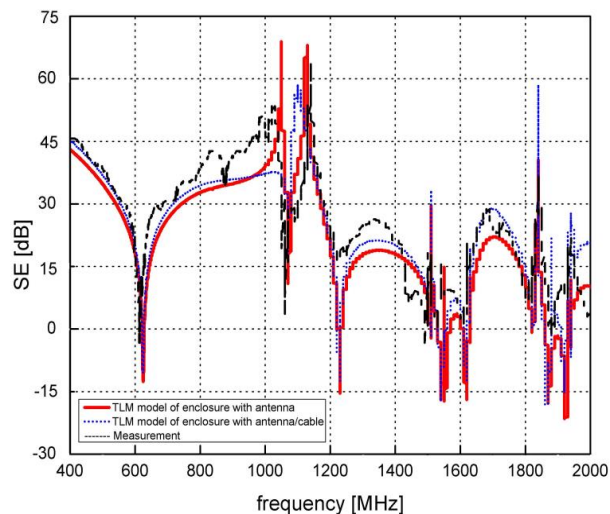


Fig. 17. SE of enclosure with three apertures (50x10 mm) on the front wall-TLM models of enclosure with antenna/cable and with antenna and measurements [4].

From Figs. 15-17 it can be noticed that in the case when antenna and cable influences are taken into account, the results for the SE are similar to the case when only physical presence of the dipole antenna in the enclosure is taken into account. However, in some parts of considered frequency range, TLM model of enclosure with antenna/cable provides slightly better agreement with the experimental results [4].

IV. CONCLUSION

In this paper, a numerical model based on TLM method with compact wire description is used to calculate the SE of metal enclosure with dipole antenna inside. The modeling case is in line with practical measurement conditions for SE characterization. Physical dimensions of dipole antenna and its cable connection are considered with respect of their influence on the level of EM field detected by the antenna. The obtained results confirm that the antenna presence affects the distribution of the EM field within the enclosure, and thus also the SE parameter value. Therefore, this impact has to be taken into account during the experimental SE characterization in order to correctly estimate the shielding properties of metal enclosure. Future research will comprise of more detailed analysis of this impact in order to empirically derive a factor that should correct the measured level of SE due to antenna and other equipment presence inside the enclosure.

ACKNOWLEDGMENT

This work has been partially supported by the Ministry for Education, Science and Technological Development of Serbia, project number TR32052.

REFERENCES

- [1] C. Christopoulos, "Principles and techniques of electromagnetic compatibility," *CRC Press*, 2007.
- [2] H. A. Mendez, "Shielding theory of enclosures with apertures," *IEEE Trans. Electromagn. Compat.*, vol. 20, no. 2, pp. 296-305, 1978.
- [3] M. P. Robinson, T. M. Benson, C. Christopoulos, J. F. Dawson, M. D. Ganley, A. C. Marvin, S. J. Porter, and D. W. P. Thomas, "Analytical formulation for the shielding effectiveness of enclosures with apertures," *IEEE Trans. Electromagn. Compat.*, vol. 40, no. 3, pp. 240-248, 1998.
- [4] J. Shim, D. G. Kam, J. H. Kwon, and J. Kim, "Circuitual modeling and measurement of shielding effectiveness against oblique incident plane wave on apertures in multiple sides of rectangular enclosure," *IEEE Trans. Electromagn. Compat.*, vol. 52, no. 3, pp. 566-577, 2010.
- [5] L. J. Nuebel, J. L. Drewniak, R. E. DuBroff, T. H. Hubing, and T. P. Van Doren, "EMI from cavity modes of shielding enclosures-FDTD modeling and measurements," *IEEE Trans. Electromagn. Compat.*, vol. 42, no. 1, pp. 29-38, 2000.
- [6] S. Ali, D. S. Weile, and T. Clupper, "Effect of near field radiators on the radiation leakage through

- perforated shields,” *IEEE Trans. Electromagn. Compat.*, vol. 47, no. 2, pp. 367-373, 2005.
- [7] B. L. Nie, P. A. Du, Y. T. Yu, and Z. Shi, “Study of the shielding properties of enclosures with apertures at higher frequencies using the transmission-line modeling method,” *IEEE Trans. Electromagn. Compat.*, vol. 53, no. 1, pp. 73-81, 2011.
- [8] N. Dončov, B. Milovanović, and Z. Stanković, “Extension of compact TLM air-vent model on rectangular and hexagonal apertures,” *Applied Computational Electromagnetic Society (ACES) Journal*, vol. 26, no. 1, pp. 64-72, 2011.
- [9] V. Milutinović, T. Cvetković, N. Dončov, and B. Milovanović, “Analysis of enclosure shielding properties dependence on aperture spacing and excitation parameters,” *In Proceedings of the IEEE TELSIKS Conference*, Niš, Serbia, vol. 2, pp. 521-524, 2011.
- [10] J. Joković, B. Milovanović, and N. Dončov, “Numerical model of transmission procedure in a cylindrical metallic cavity compared with measured results,” *Int. Journal of RF and Microwave Computer-Aided Engineering*, vol. 18, no. 4, pp. 295-302, 2008.
- [11] A. J. Wlodarczyk, V. Trenkic, R. Scaramuzza, and C. Christopoulos, “A fully integrated multiconductor model for TLM,” *IEEE Trans. Microwave Theory Tech.*, vol. 46, no. 12, pp. 2431-2437, 1998.
- [12] T. Dimitrijević, J. Joković, B. Milovanović, and N. Dončov, “TLM modeling of a probe-coupled cylindrical cavity based on compact wire model in the cylindrical mesh,” *Int. Journal of RF and Microwave Computer-Aided Engineering*, vol. 22, no. 2, pp. 184-192, 2012.
- [13] C. Christopoulos, “The transmission-line modelling (TLM) method,” *IEEE/OUP Series*, Piscataway, NJ, 1995.

Tatjana Cvetković graduated in 1989 at the Military-Technical Faculty, in Zagreb, Croatia, with the Department of Electronics and Telecommunications. Doctoral studies at the University of Niš, Faculty of Electronics, Department of Telecommunications, enrolled in 2008. She is employed in the Republic Agency for Electronic Communications, for activities related to the regulations in the area of electronic communications. She is an author and co-author of many conference works in the field of analyzing and calculation of shielding effectiveness of metal enclosures, and also in fields of regulation, realization and quality of electronic communication services.

Vesna Milutinović graduated in 2000 at the Faculty of Electronics in Niš, with the Department of Electronics and Telecommunications. Doctoral studies at the Faculty of Electronics in Niš, Department of Telecommunications, under the supervision of Professor Bratislav Milovanović, enrolled in October 2008. She has worked in planning, development and design of telecommunication networks. Since April 2007 she has been employed in RATEL for activities related to the control of radio communications. The author works in the field of telecommunication networks and systems.

Nebojša Dončov received the Dipl.-Ing. degree in Electrical Engineering and Ph.D. degree in Telecommunication Engineering from the University of Niš, Niš, Serbia in 1995 and 2002, respectively.

From 1998 to 2001, he was a Research Assistant with the Faculty of Electronic Engineering, University of Niš. From 2001 to 2004, he was a Research and Development Engineer with the Electromagnetics Division of Flomerics Ltd., Nottingham, UK. Since 2004, he has been with the Department of Telecommunications, Faculty of Electronic Engineering, University of Niš, Serbia where he is now a Full Professor. His research interests include computational and applied electromagnetics with a particular emphasis on TLM and network methods applications in microwaves and EMC.

Dončov was a recipient of the International Union of Radio Science (URSI) Young Scientist Award in 2002.

Bratislav Milovanović received the Dipl.-Ing., M.Sc. and Ph.D. degrees from the Faculty of Electronic Engineering, University of Nis, Serbia, in 1972, 1975 and 1979, respectively.

From 1972 onwards he was promoted, with the Faculty of Electronic Engineering to all academic positions to Full Professor (1990). He was the Head of the Department of Telecommunications in the period from 1994-2000 and 2004-2010, and the Dean of the Faculty of Electronic Engineering from 1994-1998. Also, he was President of Serbia and Montenegro IEEE MTT Chapter from 2004-2008. His present research work is in the field of telecommunications, particularly in the field of microwave theory and techniques, computational electromagnetic and neural networks applications. He is a General Chairman of series of IEEE TELSIKS conferences, a Member of Serbian Scientific Society since 1999, a Full Member of the Academy of Engineering Sciences of Serbia and Montenegro since 2000, President of national MTT Society since 2002.

Milovanović's awards and honors include the Octobar Prize of the City of Niš, the Annual Prizes of

Radio Television of Serbia, the Distinguished Prize (YU IEEE Society for Microwave Technique and Technology), the Diplomas of Academy of Engineering Sciences of Serbia and Montenegro, the Tesla Award (Nikola Tesla foundation in Serbia) and a number of certificates of appreciation.